Journal of Molecular Liquids 346 (2022) 117112

Contents lists available at ScienceDirect

Journal of Molecular Liquids

journal homepage: www.elsevier.com/locate/molliq

Asphaltenes as novel thermal conductivity enhancers for liquid paraffin: Insight from *in silico* modeling

Artyom D. Glova [a], Victor M. Nazarychev [a], Sergey V. Larin [a], Alexey V. Lyulin [a,b], Sergey V. Lyulin [a], Andrey A. Gurtovenko [a,*]

[a] Institute of Macromolecular Compounds, Russian Academy of Sciences, Bolshoi Prospect V.O. 31, St. Petersburg 199004, Russia
[b] Soft Matter and Biological Physics Group, Technische Universiteit Eindhoven, P.O. Box 513, 5600 MB Eindhoven, the Netherlands

ARTICLE INFO

Article history:
Received 22 May 2021
Revised 6 July 2021
Accepted 26 July 2021
Available online 30 July 2021

Keywords:
Paraffins
Organic phase-change materials
Asphaltenes
Thermal conductivity enhancement
Computer modeling
Molecular dynamics

ABSTRACT

The practical use of paraffin and other organic phase-change materials for heat storage is largely limited by their low thermal conductivity. In this paper we employed 60 microsecond-long atomic-scale computer simulations to explore for the first time whether the asphaltenes, natural polycyclic aromatic hydrocarbons, can be used as thermal conductivity enhancers for paraffin. We focused on a simple model molecule of asphaltene (a polycyclic aromatic core decorated with the peripheral alkane chains) and showed that the asphaltenes of such molecular architecture are not able to improve the thermal conductivity of paraffin. This is most likely due to the steric constraints imposed by the peripheral alkane groups, which prevent formation of the extended ordered asphaltene aggregates. To overcome this, we proposed a possible chemical modification of the asphaltene molecules through removing the peripheral alkane groups from their aromatic cores; this could be achieved e.g. by thermal cracking (dealkylation) of asphaltenes. It turns out that such a chemical modification drastically changes the situation: the modified asphaltenes form extended columnar aggregates which can serve as thermal conduction paths, considerably enhancing the thermal conductivity of a liquid composite sample. This effect, however, vanishes upon cooling because the columnar extended stacks of chemically modified asphaltenes transform into the helical twisted structures, which reduces the overlap of adjacent asphaltenes in aggregates. Importantly, all the simulations have been carried out with two different all-atom force fields. We have demonstrated that both computational models give qualitatively similar results. Overall, our findings clearly show that chemically modified asphaltene molecules can be considered as promising carbon-based thermal conductivity enhancers for liquid paraffin; this result can be used for optimizing the paraffin-based thermal energy storage systems.

1. Introduction

The rational use of thermal energy has become an increasingly important issue in view of the environmental protection and energy conservation. To overcome the unnecessary waste of thermal energy in industry and households, it is highly desirable to have means to control the energy distribution by storing and releasing the thermal energy when it is supplied and demanded [1]. One of the possible approaches to achieve this is to use the phase-change materials (PCM). The PCMs are able to adsorb and release heat by phase changes (e.g. by transition from the solid phase to the liquid one and vice versa) and can therefore be used for the thermal energy storage [2,3]. PCMs are characterized by rather large latent heat of fusion, chemical stability, and relatively low cost [4].

The focus of the present study is on paraffins, a typical representative of organic PCMs [1,5]. Paraffins consist of a mixture of *n*-alkane chains of various length. The average length of the hydrocarbon chains is a key factor for tuning the paraffin-based PCMs: by varying the chain length, one can adjust the phase transition temperature to a well-defined value between 6 °C and 76 °C, depending on the requirements for the PCM's operating temperature range [3,5]. Other important advantages of paraffins include high energy storage density, thermal and chemical stability, nontoxicity, abundance, and low cost [1,6]. All these make paraffins an excellent candidate for using in heat storage devices.

In general, the practical applications of all (non-metallic) PCMs have a common bottleneck: low thermal conductivity [7]. This

* Corresponding author.
E-mail address: a.gurtovenko@biosimu.org (A.A. Gurtovenko).

https://doi.org/10.1016/j.molliq.2021.117112
0167-7322/

implies the low rate of charging and discharging the PCM-based heat storage devices, leading to their insufficient performance. We note that organic PCMs are characterized by the lowest thermal conductivity among the (non-metallic) PCMs [8]. In this regard, paraffins are not an exception: their thermal conductivity is very low and amounts to approximately 0.2 Wm^{-1} K^{-1} [2]. Therefore, the main issue in practical applications of paraffins (and other PCMs) is directly related to the thermal conductivity enhancement.

One of the common approaches for enhancing the thermal conductivity of a material is adding the substances with high thermal conductivity [7,9,10]. These substances can form thermal conduction paths, accelerating thereby the heat transfer. Among others, carbon-based nano-additives (such as graphene or carbon nanotubes) are very promising due to their outstanding thermal conductivity, structural stability, large surface area, and low density [11]. The latter is especially important as excessively high content of additives can reduce considerably the heat storage capacity of PCMs. In particular, it was shown that adding 0.3 wt% graphene to beeswax increases the thermal conductivity of a composite system by an order of magnitude (from 0.25 to 2.89 W/m K) [12]. Such an extremely efficient graphene-induced enhancement of the thermal conductivity of organic PCMs is due to the presence of a planar conjugated hexagonal lattice of carbon atoms [13]. However, despite the proven ability of graphene to enhance thermal conductivity, its practical application is very limited due to high cost [14], which makes PCM/graphene systems prohibitively expensive.

Such situation calls for carbon-based additives that would be much cheaper than graphene or carbon nanotubes. At the same time, these additives should preserve some of the important chemical features of graphene such as e.g. a two-dimensional carbon lattice. Among other candidates, asphaltenes, natural polycyclic aromatic hydrocarbons meet both these criteria.

Asphaltenes represent low-cost byproducts of deep oil refining [15]: depending on the source, crude oil comprises up to 20% of asphaltenes [16–18]. During refining, the asphaltenes have to be removed from the crude oil because they have a negative impact on the economic value of oil (increased oil viscosity and, correspondingly, low fluid mobility, plugging of pipelines, undesired color changes etc) [19,20]. Most these "negative" features stem from the aggregation of asphaltene molecules. Although molecular architecture of asphaltenes varies considerably, it is known that an asphaltene molecule can consist of one or several cross-linked units; each unit comprises moderately large polycyclic aromatic core with short peripheral alkane chains [15], see Fig. 1 for a schematic representation of a model asphaltene molecule. Therefore, the above mentioned asphaltene aggregation is most likely driven by the π-π interactions between asphaltenes' polycyclic disk-like cores [16,19]. And more importantly, it is these cores that make asphaltenes resemble small graphene fragments.

This resemblance to graphene allows one to consider asphaltenes as a novel promising class of carbon nanofillers. Indeed, asphaltenes were recently used as fillers in polymer nanocomposites with improved thermal and mechanical properties [21–26]. Furthermore, due to their electronic conductivity, it was proposed to use asphaltenes in bulk heterojunction solar cells as potential acceptor nanofillers [27–29]. However, to the best of our knowledge, the impact of asphaltenes on the thermal conductivity of phase-change materials has never been studied (neither experimentally, nor theoretically).

To meet lack of such studies, we report here the first atomic-scale molecular dynamics simulations of paraffin samples filled with asphaltene molecules. The use of the state-of-the-art computer modeling allows us to reveal the impact of asphaltenes on the paraffin's thermal conductivity and – more importantly – unlock the underlying molecular mechanisms. The latter is not accessible by most existing experimental techniques. As we proceed to show, asphaltene molecules are able to enhance the thermal conductivity of liquid paraffin, provided that the asphaltenes are chemically modified through cutting off peripheral alkane chains from their aromatic cores. These findings could be employed for optimizing the thermal energy storage systems based on paraffins.

2. Methods

2.1. System description

We performed atomic-scale molecular dynamics simulations of the paraffin samples filled with asphaltene molecules. In general, paraffins represent a mixture of alkane chains of various lengths. However, in our study we focus on a simplified situation when all hydrocarbon chains are of the same length. We chose to consider *n*-eicosane ($C_{20}H_{42}$), see Fig. 1(a). The phase transition temperature of this *n*-alkane is close to the physiological temperature (37 °C), which makes it one of the most promising paraffins for the use in domestic heat storage devices [3]. Furthermore, recently the structural and thermal properties of *n*-eicosane were systematically studied through atomistic computer modeling [31–33].

As for the asphaltenes, a choice of a model molecule is far from trivial due to a great variety of possible asphaltene's molecular architectures [15]. This molecular polydispersity of asphaltenes makes their computer modeling a very challenging issue [34,35]. As mentioned in the Introduction, an asphaltene molecule can comprise one (the so-called "island" type [15,36]) or several (an "archipelago" type [37]) polycyclic aromatic cores. Our strategy of choosing an asphaltene model was based on two considerations: (1) an asphaltene's molecular architecture should be as simple as possible and (2) a model molecule should be previously studied. These principles brought us to the asphaltene structure depicted in Fig. 1(b). This model asphaltene molecule has a polycyclic core of 9 rings (including 7 aromatic rings and 1 sulfur heteroatom) and several peripheral alkane groups; it was first suggested by Mullins [15] and later optimized by Li and Greenfield [30]. The molecule was shown to comply with the asphaltene's definition, which implies insolubility in heptane and solubility in toluene [38]. Furthermore, the asphaltene of such molecular architecture was employed in earlier studies of the water–oil interface [39] and asphalt [30,40,41].

In general, it is well established that the π–π interactions between the planar polycyclic cores are able to promote the heat transfer in the system [42,43]. However, according to the Yen-Mullins model of asphaltene aggregation and experimental data [36,44,45], asphaltenes form relatively loose aggregates that contain disordered stacks of molecules. This is most likely due to the steric interactions between the peripheral alkane groups, which prevent formation of the extended and ordered stacks of asphaltenes [15,36]. On the other hand, the polycyclic aromatic cores of asphaltenes have much in common with the discotic liquid crystalline molecules, such as coronene and hexabenzocoronene, which normally pack in ordered bundles of columnar rod-like stacks [46]. Therefore, a possible strategy for enhancing the π–π interactions of asphaltenes (and correspondingly for promoting their ordered packing) would be the removal of the peripheral alkane chains from the aromatic cores of asphaltenes. Experimentally this can be achieved by cracking (dealkylation) of asphaltenes [47,48]. In our study we explore such a possibility and consider – in addition to the asphaltenes shown in Fig. 1(b) – chemically modified asphaltenes obtained from the original molecule by cutting off the peripheral alkane groups and transforming one ring of the core

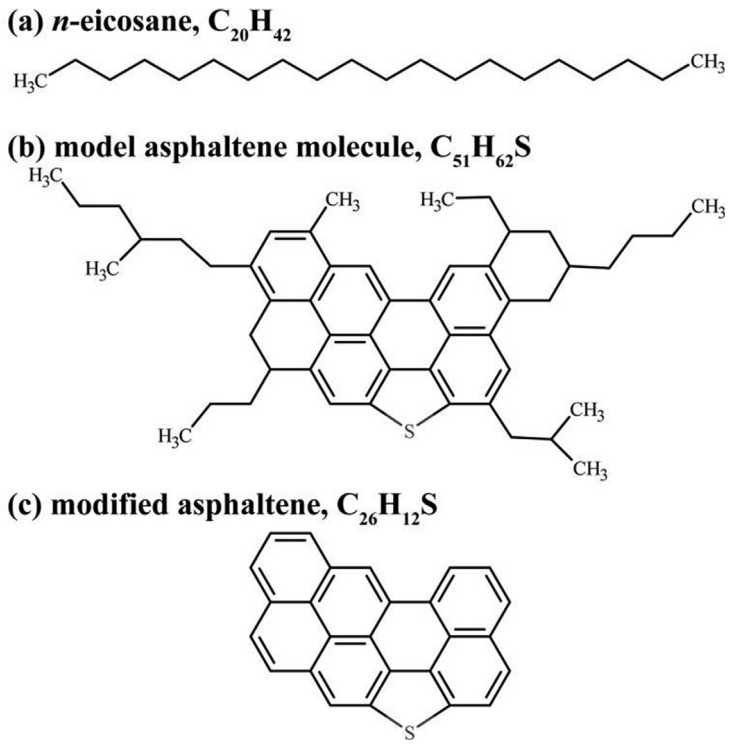

Fig. 1. The chemical structures of the constituents of the considered paraffin-asphaltene systems: (a) *n*-eicosane, (b) a model asphaltene molecule [15,30], and (c) a model asphaltene with peripheral alkane chains cut off.

into the aromatic one, see Fig. 1(c). This makes it possible to shed light on the role of the peripheral alkane chains in asphaltene aggregation and asphaltene-induced changes in the thermal conductivity.

2.2. Preparation of paraffin-asphaltene samples

Each paraffin-asphaltene system represented a mixture of 500 *n*-eicosane chains (N_{par}) and a certain number of asphaltene molecules, N_{asp} (either unmodified or modified). The number of asphaltenes was systematically varied from 21 to 396, see Table 1 for the list of all the simulated systems. This way we preserved the polyaromatic content in the systems with two types of asphaltenes (Figs. 1(b) and 1(c)). However, the weight fractions of asphaltenes (C_{asp}) are different: they range from 5 to 50 wt% for asphaltenes without peripheral alkane groups (the PAR-ASP-mod systems in Table 1) and from 9.5 to 66.4 wt% for unmodified asphaltenes (the PAR-ASP systems). The total number of atoms in the systems varied from 32 000 to 76 000.

Note that we consider a wide range of asphaltene concentrations up to very large values (66.4 wt% and 50 wt% for systems with unmodified and modified asphaltenes, respectively). This is usual for the computer modeling that is designed to explore the limits that are hard to achieve in experiments. However, when it comes to practical applications of thermal conductivity enhancers, it should be kept in mind that such high content of additives significantly reduces the heat storage capacity of phase-change materials [10].

Preparation of the initial configurations of paraffin samples filled with the asphaltenes closely followed the procedure outlined in ref [31]. In brief, randomly oriented *n*-eicosane chains and asphaltene molecules were initially put in a cubic simulation box. The generated system was compressed for 5 ns with a pressure of 50 bar at a temperature of 450 K. The temperature was chosen to be well above the phase transition temperature of *n*-eicosane (310 K), ensuring thereby that the simulated paraffin-asphaltene samples are in the liquid state. After the compression, the pressure was reduced to 1 bar and the liquid paraffin-asphaltene systems were simulated for 1 μs, see Table 1. The anal-

Table 1
Simulated paraffin-asphaltene systems.

System	N_{par}	N_{asp}	C_{asp} [wt%]	Simulations of liquid samples[a] at 450 K [ns]	Cooling-rate simulations[a] [ns]
PAR-ASP-21	500	21	9.5	1000	21 × 100
PAR-ASP-44	500	44	18	1000	21 × 100
PAR-ASP-99	500	99	33.1	1000	21 × 100
PAR-ASP-214	500	214	51.7	1000	21 × 100
PAR-ASP-396	500	396	66.4	1000	21 × 100
PAR-ASP-mod-21	500	21	5	1000	21 × 100
PAR-ASP-mod-44	500	44	10	1000	21 × 100
PAR-ASP-mod-99	500	99	20	1000	21 × 100
PAR-ASP-mod-214	500	214	35	1000	21 × 100
PAR-ASP-mod-396	500	396	50	1000	21 × 100

[a] Each simulation was performed with 2 force fields (GAFF and CHARMM).

ysis of the autocorrelation functions of the distances between centers of mass of the asphaltenes showed that the initial equilibration of the paraffin-asphaltene systems takes approximately 100 ns, see Fig. S1 of the Supporting Information. Therefore, the last 900 ns of MD trajectories were considered as production runs and were used for the analysis of the properties of the liquid samples.

To study the impact of the asphaltenes on the paraffin's thermal conductivity in the crystalline state, all liquid paraffin-asphaltene samples were cooled down to T = 250 K. In line with refs [31,32], we performed a series of cooling-rate simulations, in which the cooling was carried out in a stepwise manner from 450 to 250 K with steps of 10 K; at each cooling step (21 steps in total) the system was simulated for 100 ns, see Table 1.

2.3. Simulation details

All the molecular dynamic simulations of paraffin-asphaltene systems were repeated twice with GAFF [49] and CHARMM36 [50,51] all atom force fields. In general, the choice of a proper force field is dictated by the ability of a model to correctly describe the target physical quantity. As a primary focus of our study is on the thermal conductivity, in this study we employ the GAFF force field that was proved to show the best performance for thermal conductivity of *n*-eicosane among 10 atomistic force fields [33]. In addition, we decided to perform all the MD simulations with the CHARMM36 force field, another force field that also performed well for *n*-eicosane [33]. Furthermore, both GAFF and CHARMM36 force fields showed reasonable performance in MD simulations of asphaltenes [38,52–57]. The use of two different force fields allows us to minimize the possible simulation artifacts and to test the robustness of the computational results against the theoretical models employed.

The GROMACS simulation package [58] was used for sample preparation, the simulations of the liquid paraffin-asphaltene systems, and for the cooling-rate simulations. For *n*-eicosane, the initial structures and the force field parameters were taken from our previous studies [31–33]. In the case of the asphaltene molecules (Figs. 1(b) and 1(c)) we used the ACPYPE [59,60] and CHARMM-GUI [61,62] tools for GAFF and CHARMM force fields, respectively. A complete description of GAFF and CHARMM models of asphaltenes is presented in the Supporting Information. During the sample preparation both temperature and pressure were controlled with the use of the Berendsen scheme [63]. For simulations of liquid samples and for the subsequent cooling we switched to the Nose-Hoover thermostat [64,65] and the Parrinello-Rahman barostat [66]. The P-LINCS algorithm [67] was employed to constrain all bonds with hydrogen atoms. The electrostatic interactions were handled by the particle mesh Ewald method [68]. Periodic boundary conditions were applied in all three directions. The time step was 2 fs. The accumulated simulation time for the paraffin-asphaltene systems amounted to 62 microseconds, see Table 1.

2.4. Calculation of thermal conductivity

The thermal conductivity was evaluated with the use of the LAMMPS simulation package (version from 15 Apr 2020) [69]. Prior actual calculations, we converted the paraffin-asphaltene samples from GROMACS to LAMMPS representation using the approach described in detail in our previous study [33]. To calculate the coefficient of thermal conductivity κ, we employed the equilibrium molecular dynamics simulations (EMD) [70] which were shown to outperform the non-equilibrium approaches for paraffin samples of a comparable size [33]. The EMD method computes the value of the coefficient of thermal conductivity κ from the heat flux autocorrelation function (HFACF) using the Green-Kubo relation [71,72]. In practice, we performed short, 1 ns-long EMD simulation runs of the paraffin-asphaltene samples in the NVE ensemble to extract the heat flux. The HFACFs were then computed with the use of the correlation time of 10 ps [73]. Finally, the calculated HFACFs were used for evaluating the coefficient of thermal conductivity κ, which was averaged over the last 500 ps of EMD trajectories [33].

3. Results and discussion

3.1. Impact of asphaltenes on thermal conductivity

The main focus of our study is on the asphaltene-induced impact on the thermal conductivity of paraffin. Paraffin, being an organic phase-change material, adsorb and release heat by phase changes (melting and crystallization). During the charging phase paraffin is in a solid (crystalline) state; upon charging it undergoes a phase transition and becomes a liquid. The thermal conductivity of crystalline paraffin controls the charging rate, while the properties of a liquid paraffin define the rate of discharging of the paraffin-based heat storage devices. Thus, the thermal conductivity of the paraffin-asphaltene samples in both liquid and crystalline states matters.

Initially, all the paraffin-asphaltene systems were prepared and equilibrated in the liquid state at T = 450 K. In Figs. 2 and S2 we show representative snapshots of paraffin-asphaltene systems at T = 450 K for CHARMM and GAFF simulations, respectively. As one can conclude from visual inspection of the snapshots, asphaltene molecules tend to form aggregates; this effect is more noticeable for the asphaltene molecules without peripheral alkane chains, see the bottom rows in Figs. 2 and S2.

In order to obtain the crystalline samples, we performed stepwise cooling of the systems. The experimental value of the phase transition for *n*-eicosane is 310 K [3]. Corresponding computational values slightly depend on a force field and amount to 320 and 330 K for CHARMM and GAFF force fields, respectively [31,32]. Therefore, the cooling of samples was performed in the range from 450 to 250 K, i.e. to the temperature that is much lower than the crystallization point of *n*-eicosane. In Fig. 3 and Fig. S3 we show the temperature dependence of the mass density ρ of the paraffin-asphaltene samples for the two force fields employed. As the outcome of simulations turned out to be very similar for both force fields, the density of samples will be discussed for the CHARMM simulations only.

First off, one can observe a systematic increase in the density of paraffin-asphaltene samples with asphaltene concentration; for all fractions of asphaltenes the mass density of the corresponding systems exceeds that for pure (unfilled) paraffin. This implies that asphaltene molecules aggregate with formation of structures whose density is higher than that of a pure paraffin. Moreover, the character of the observed density growth depends on the chemical structure of asphaltenes. The observed density increase turns out to be more pronounced for asphaltenes without peripheral alkane chains, i.e. the chemical modification of asphaltenes promotes formation of denser aggregates, see Fig. 3. Furthermore, for the PAR-ASP-mod systems the $\rho(T)$-curves are systematically shifted to the larger values over the entire temperature range when the asphaltene fraction increases. Such an additive increment in the density could be explained by the fact that increasing asphaltene fraction solely leads to a growth of asphaltene aggregates, see Fig. 2. In contrast, for the unmodified asphaltenes the above-mentioned behavior is observed only in the high-temperature domain. At low temperatures, the density increase is much smaller, most likely because the unmodified asphaltenes mix rather well with paraffin chains, disrupting thereby the paraffin's crystalline

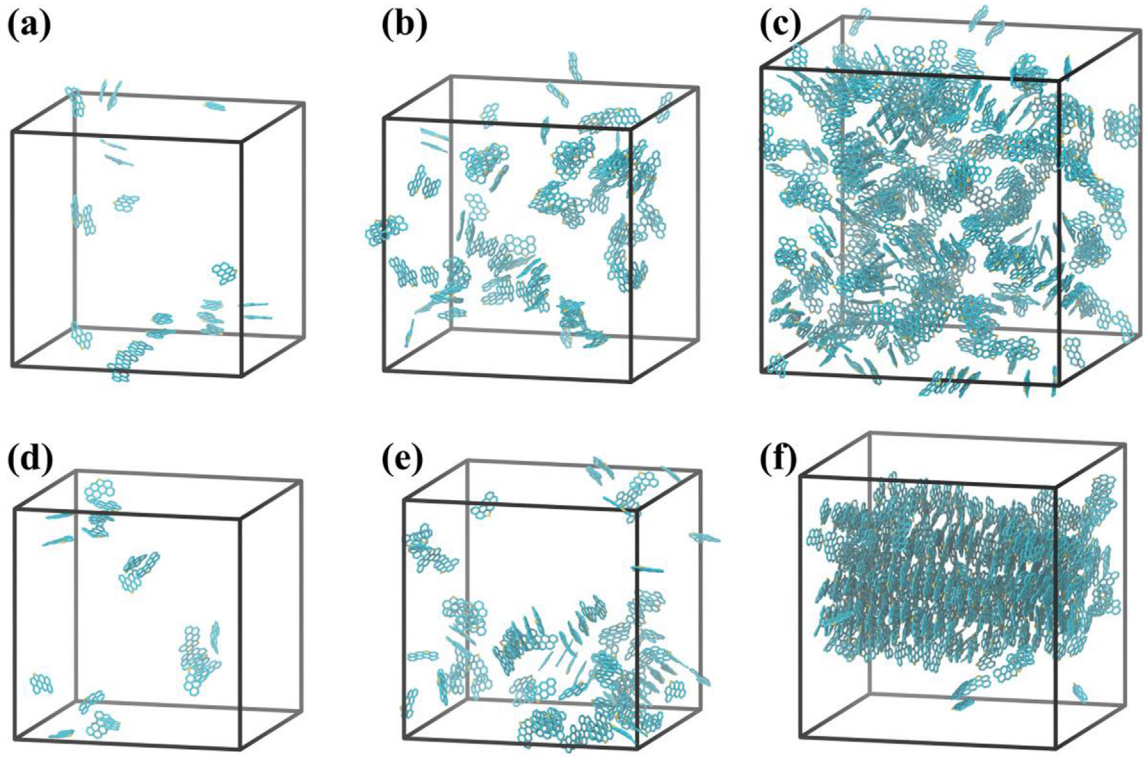

Fig. 2. Representative snapshots of paraffin-asphaltene systems at T = 450 K (CHARMM simulations). Shown are snapshots for PAR-ASP-21 (a), PAR-ASP-99 (b), PAR-ASP-396 (c), PAR-ASP-mod-21 (d), PAR-ASP-mod-99 (e), and PAR-ASP-mod-396 (f) systems. For clarity, only aromatic cores are shown for asphaltenes of both types; paraffin chains are not shown.

packing. This is partly confirmed by the lack of crystallization of the paraffin-asphaltene systems with the highest concentrations of unmodified asphaltenes: the corresponding $\rho(T)$-curves do not show an abrupt increase in the density upon cooling, see Fig. 3. It is also noteworthy that if the phase transition does exist, the corresponding crystallization temperature is not affected by the presence of asphaltenes.

After cooling down the paraffin-asphaltene samples to the temperatures that are well below the crystallization point, we compute the coefficient of thermal conductivity κ for both liquid and crystalline samples. The outcome of such calculations is shown in Fig. 4 and represents the main result of our computational study.

As is immediately evident from Fig. 4, there is a striking difference in the asphaltene-induced effect on the thermal conductivity of crystalline and liquid paraffin. At low temperatures, when most of the paraffin-asphaltene samples are in the crystalline state, asphaltenes do not improve the thermal conductivity properties of paraffin, see Fig. 4(a) and (c). Even worse, for most systems adding asphaltene molecules leads to somewhat smaller values of the thermal conductivity compared to that of an unfilled paraffin crys-

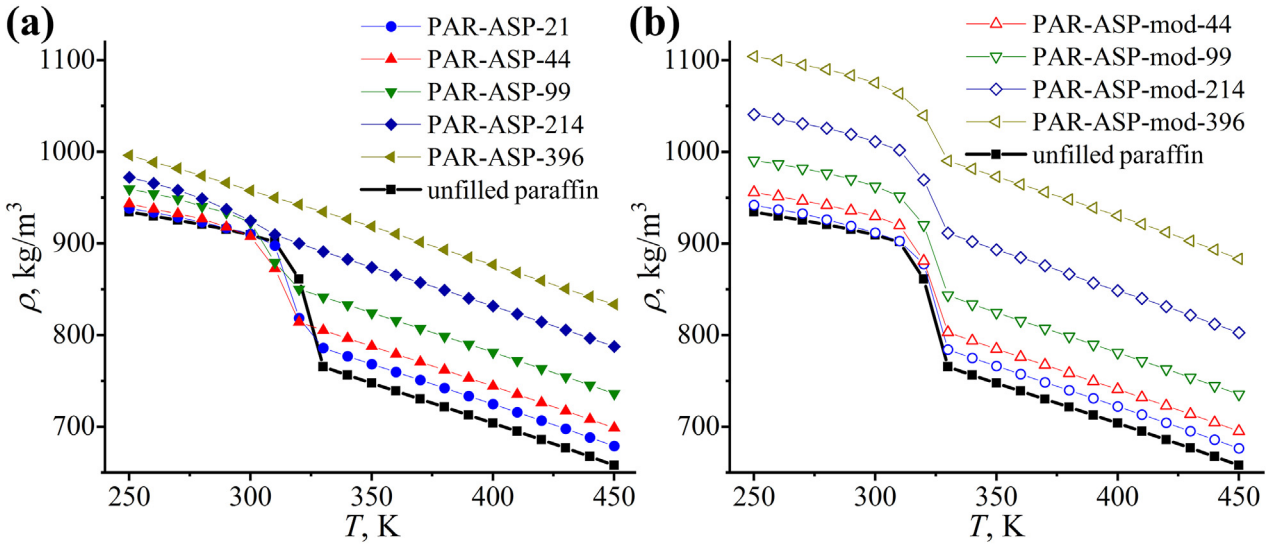

Fig. 3. Mass density ρ of the paraffin-asphaltene samples as a function of temperature T for the CHARMM force field. Shown are the results for the unmodified (a) and modified (b) asphaltenes. The data for the unfilled paraffin is taken from refs [31].

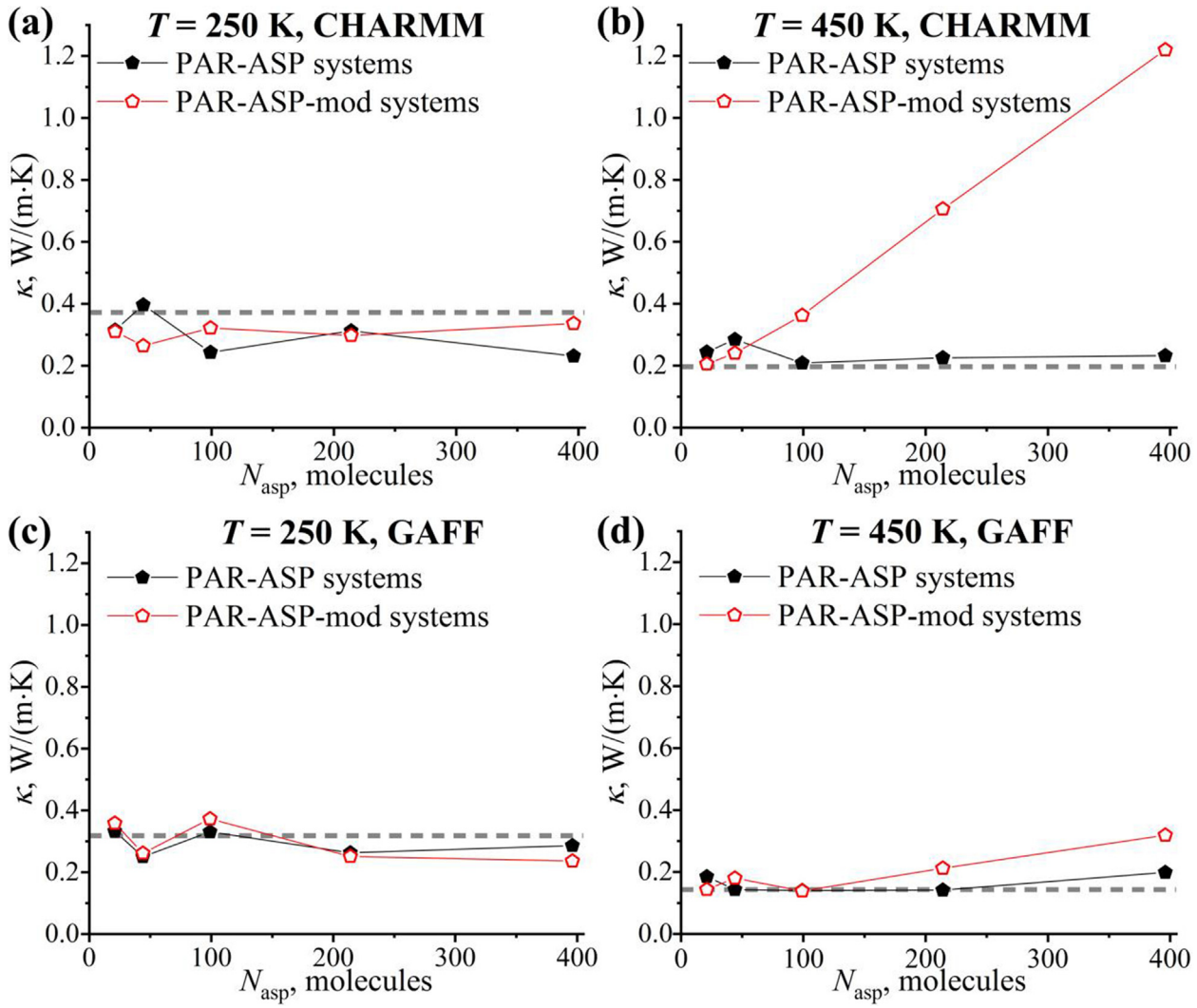

Fig. 4. The thermal conductivity coefficients κ of the simulated paraffin-asphaltene samples as a function of the number N_{asp} of asphaltene molecules in a sample at low (T = 250 K) and high (T = 450 K) temperatures. Shown are the results for CHARMM (a,b) and GAFF (c,d) simulations. The horizontal dashed lines show the κ values for the unfilled n-eicosane [33].

tal. This conclusion holds for both force fields considered and for the two types of asphaltene molecules. Note that this asphaltene's negative impact could have a different physical origin for asphaltenes with and without peripheral alkane chains. As mentioned above (see Fig. 3(a)), the unmodified asphaltenes could disrupt the packing of paraffin chains, inducing defects in the crystalline paraffin and reducing thereby the thermal conductivity. When asphaltenes are chemically modified, they seem to disrupt the paraffin crystal to a much smaller extent, see Fig. 3(b). In this case, the observed overall decrease in the thermal conductivity of the paraffin-asphaltene samples is likely because the thermal conductivity of asphaltene aggregates at T = 250 K is smaller than that of the crystalline paraffin domains.

In great contrast with the crystalline samples, adding asphaltene molecules is able to improve the thermal conductivity properties of a liquid paraffin. While this improvement is very moderate and almost vanishing for unmodified asphaltenes, the asphaltenes without peripheral alkane chains do enhance considerably the thermal conductivity of the liquid paraffin-asphaltene samples, see Fig. 4(b) and (d). Another important feature to be noticed in Fig. 4(b) and (d) is a difference in the asphaltene-induced thermal conductivity enhancement predicted by the two force fields. While both force fields show qualitative agreement with each other, quantitatively the thermal conductivity increase in CHARMM and GAFF simulations differs considerably. In particular, adding modified asphaltenes of the highest concentration (50 wt%) leads to the 6-fold and the 2-fold growth in the thermal conductivity of liquid samples for CHARMM and GAFF force fields, respectively.

Summing up, our computational findings clearly show that the modified asphaltene molecules are able to enhance the thermal conductivity of liquid paraffin. In the next Sections we will use the power of computer simulations to unlock a molecular mechanism of this thermal conductivity enhancement. In particular, we will link the thermal conductivity enhancement with the ability of modified asphaltenes to form extended ordered aggregates. Furthermore, we will show that the difference between CHARMM and GAFF simulations can directly be attributed to the strength of the interactions between asphaltene's cores in both force fields.

3.2. Aggregation of asphaltenes in liquid paraffin

As mentioned in the previous Section, the asphaltene aggregation is most likely responsible for the thermal conductivity enhancement observed in liquid paraffin-asphaltene samples. To characterize the asphaltene aggregates, we performed a cluster analysis of the asphaltene molecules in a liquid paraffin. The fol-

lowing geometric criterion was used [38]: two asphaltene molecules belong to the same aggregate if the smallest atomic distance between the asphaltenes is within a cut off radius of 0.45 nm. To treat the modified and unmodified asphaltenes on the same footing, only polycyclic aromatic cores of asphaltenes were considered in the cluster analysis [74]. After asphaltene molecules have been assigned to aggregates, one can evaluate the various structural characteristics of the asphaltene aggregation such as the average number N_{av} of asphaltenes per aggregate and the average number N_{agr} of aggregates in a system. In Fig. 5 we present the N_{av} and N_{agr} values for all the liquid paraffin-asphaltene samples considered. In addition, Fig. S4 shows the number of asphaltenes in the largest aggregate, as well as the number of free-standing (non-aggregating) asphaltenes in the system.

As is evident from Figs. 5 and S4, the aggregation behavior is quite different for asphaltene with and without peripheral alkane chains. The unmodified asphaltenes form relatively small aggregates, the number of molecules in the largest aggregate does not exceed 30 in the whole concentration range, see Fig. S4. As a result, increasing concentration of asphaltenes mainly results in the formation of new small aggregates rather than in the increase of the aggregate size, see Fig. 5. The overall uniform distribution of aggregates of unmodified asphaltenes implies that their peripheral alkane chains make the asphaltenes rather soluble in *n*-eicosane. Although the asphaltenes by definition are insoluble in heptane, our results are in line with the fact that the precipitating of asphaltenes becomes weaker when the length of *n*-alkane chains increases (*n*-eicosane is considerably longer than *n*-heptane [75]).

Cutting off the peripheral alkane chains from the asphaltene's core changes drastically the aggregation behavior of the asphaltenes. As seen from Figs. 5 and S4, the chemically modified asphaltenes form much larger aggregates compared to their unmodified counterparts. As for the average number of aggregates, it shows a non-monotonic behavior. At first, it increases moderately at small asphaltene concentrations. However, when the number of asphaltenes exceeds 100 molecules per 500 *n*-eicosane chains, the number of aggregates drops with concentration, see Fig. 5. In other words, adding more asphaltenes to the system leads to the merging of the existing aggregates rather than to the formation of new ones. Therefore, at the highest concentration all asphaltene molecules form a single "super-aggregate" in a liquid paraffin. Such a behavior can be explained by poor solubility of chemically modified asphaltenes in a liquid paraffin: removing the peripheral alkane chains makes asphaltene molecules less compatible with the paraffin chains, promoting thereby the asphaltenes' aggregation.

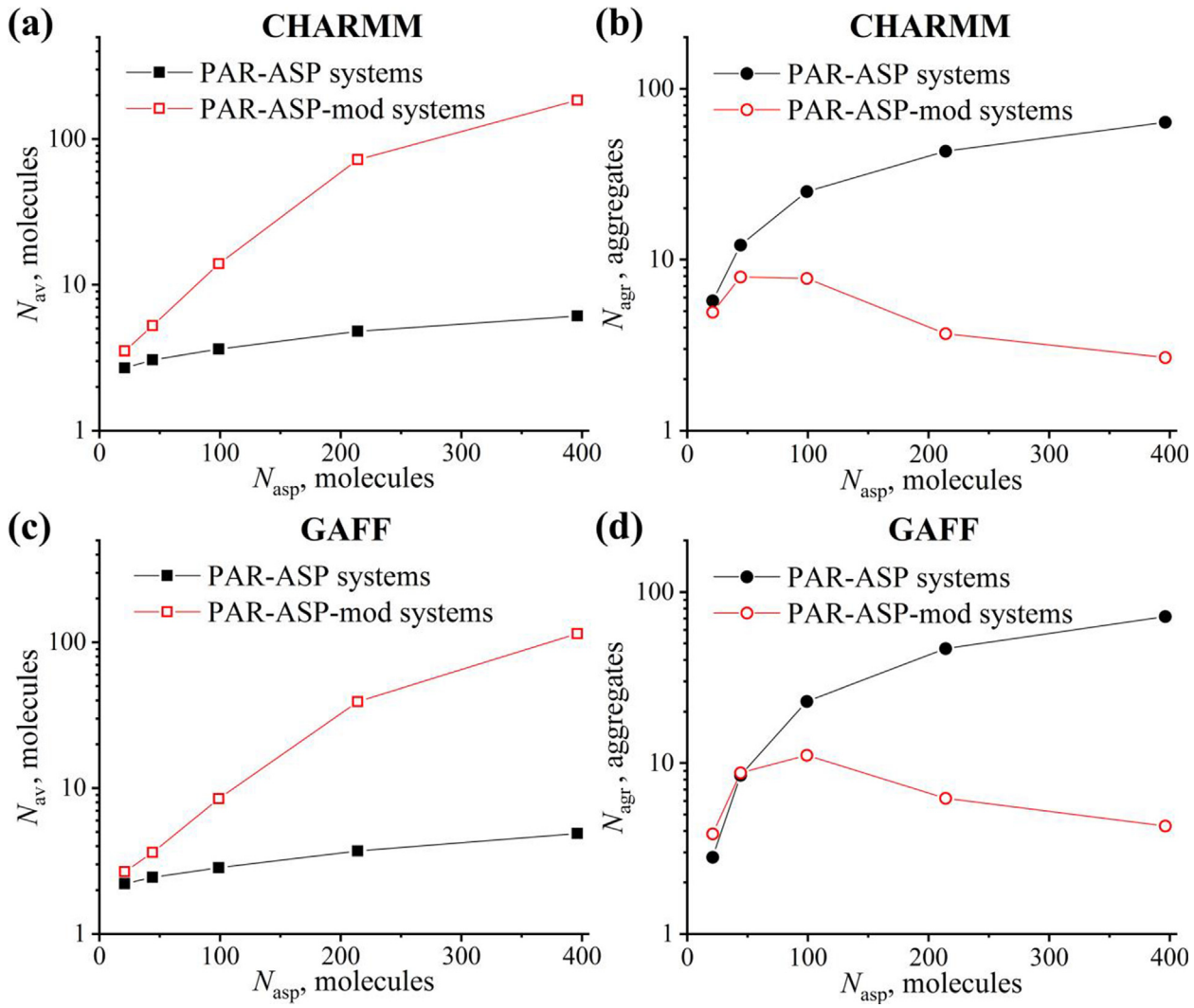

Fig. 5. The average number N_{av} of the asphaltenes per aggregate and the average number N_{agr} of the aggregates in liquid paraffin-asphaltene samples as a function of the number N_{asp} of the asphaltene molecules in a system. Shown are the results for CHARMM (top) and GAFF (bottom) force fields. The averaging is performed over 900 ns MD trajectories.

As for the comparison of two force fields, Fig. 5 shows that the aggregation behavior of the asphaltenes is qualitatively similar for both CHARMM and GAFF simulations. However, when it comes to the detailed structural organization of asphaltenes in aggregates, there are some important differences. It is these differences that led to the discrepancy in the thermal conductivity enhancements predicted by the two force fields for modified asphaltenes, see Figs. 4(b) and 4(d).

To get an insight into the microstructure of the asphaltene aggregates, we calculated the radial distribution functions (RDFs) for the centers of mass of the aromatic polycyclic cores of asphaltenes. The outcome of such calculations is shown in Fig. 6 (the CHARMM force field) and Fig. 7 (the GAFF force field) for three representative asphaltene concentrations. In CHARMM simulations the RDFs for the unmodified asphaltenes show up to 3 peaks, which is a signature of formation of stacks. Importantly, at large distances the RDF-curves approach unity, i.e. there is no long-range correlations between the asphaltene molecules, see Fig. 6. This implies a uniform distribution of small stacks of unmodified asphaltenes in liquid paraffin. In contrast, for the RDFs for asphaltenes without alkane periphery the peaks are higher, and their positions are shifted to smaller distances, implying denser asphaltene packing. The RDF-curves do not return to unity at large distances, showing the long-range order of asphaltenes, especially at high asphaltene concentrations. Therefore, the chemically modified asphaltenes preferably form large aggregates consisting of the extended ordered asphaltene stacks.

The character of RDFs in GAFF simulations turned out to differ considerably from what was observed for the CHARMM force field. For asphaltenes with peripheral alkane chains the RDFs have only one peak, so that the asphaltene aggregates, being uniformly distributed in a sample, are less ordered as compared to CHARMM simulations, see Figs. 6 and 7. In turn, the chemical modification of asphaltenes promotes formation of the more ordered structures (stacks), as visualized by the change in the RDF-curves in Fig. 7. However, in this case the RDFs show a single main peak, so that these stacks are rather small. Combining this observation with the fact that the modified asphaltenes form just a few aggregates at high asphaltene concentrations (Fig. 5(d)), one can conclude that in GAFF simulations a large "super-aggregate" represents an ensemble of small ordered stacks (cf. with extended ordered asphaltene stacks in CHARMM simulations).

The observed force field-specific difference in the asphaltene aggregation can also be illustrated through the mobility of the asphaltene molecules in a liquid paraffin. To characterize the mobility, we evaluated the diffusion coefficients of the asphaltenes for all paraffin-asphaltene systems; the results are presented in Table S1. It is seen that the diffusion coefficients of asphaltenes are systematically larger in GAFF simulations for both modified and unmodified asphaltenes. This important finding confirms that the asphaltenes in GAFF simulations form stacks that are smaller and less ordered as compared to CHARMM simulations. Remarkably, for the highest asphaltene concentration the mobility of modified asphaltenes is an order of magnitude lower, when the CHARMM force field is employed, see Table S1. Such a slowing down implies that in this case the majority of the asphaltene molecules in the system are organized in a single well-ordered "super-aggregate".

All in all, the radial distribution functions (Figs. 6 and 7) along with the results on the asphaltene mobility allow us to directly link the difference in the thermal conductivity enhancement predicted by different force fields (Fig. 4) with the structural organization of chemically modified asphaltenes in a liquid paraffin. The formation of stacks of asphaltene molecules is known to be controlled by the π-π interactions between their aromatic cores [44]. Our computational findings show that these interactions are noticeably stronger in the case of the CHARMM force field, leading to the formation of extended columnar-like stacks of the modified asphaltenes. In turn, in GAFF simulations the π-π interactions are much weaker, so that the asphaltene stacks are small and the corresponding

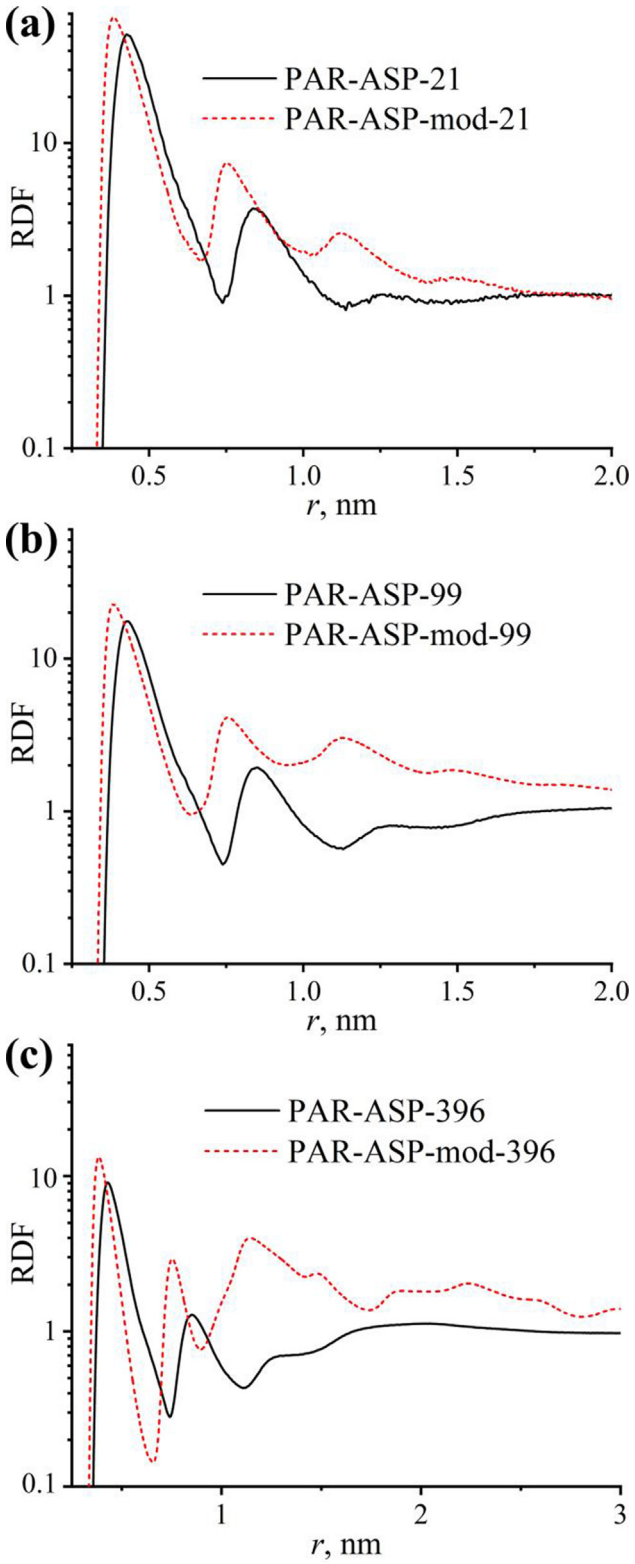

Fig. 6. The radial distribution functions (RDF) for the centers of mass of aromatic polycyclic cores of asphaltenes in liquid paraffin-asphaltene samples. Shown are the results for the CHARMM force field.

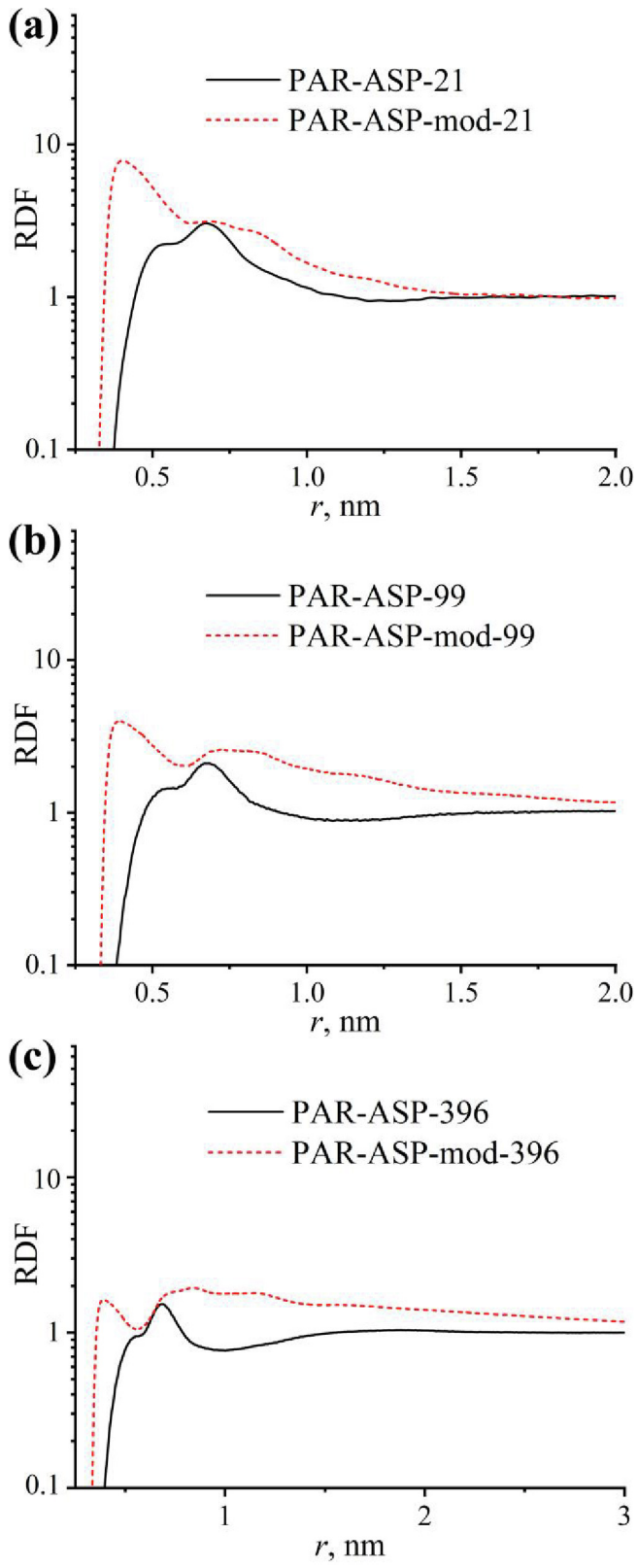

Fig. 7. The radial distribution functions (RDF) for the centers of mass of aromatic polycyclic cores of asphaltenes in the liquid paraffin-asphaltene samples. Shown are the results for the GAFF force field.

thermal conductivity enhancement is less pronounced. It should be emphasized that the choice of a proper force field for describing the asphaltene aggregation is far from trivial. The asphaltenes without peripheral alkane groups resemble coronene molecules which are known to form extended columnar aggregates [46,76]. Therefore, one might speculate that the CHARMM force field provides a better description. However, given the absence of the experimental data on the aggregation of chemically modified asphaltenes, a definitive choice of the best computational model is currently not feasible.

3.3. Putative mechanism of asphaltene-induced thermal conductivity enhancement

To conclude, we focus on the puzzling behavior of the paraffin-asphaltene composite systems upon cooling: the thermal conductivity enhancement due to the chemically modified asphaltenes vanishes during liquid-to-solid phase transition, see Fig. 4. We note that in most cases the trend is quite opposite. For instance, according to experimental data [77,78], the coefficient of thermal conductivity of *n*-eicosane increases from 0.117 W/(m K) in the liquid state (T = 453 K) to 0.413 W/(m K) in the crystalline phase (T = 275 K): the crystallization of paraffin samples enhances the ordering of alkane chains and promotes the phonon transfer.

For our purposes we consider in detail CHARMM simulations of the PAR-ASP-mod-396 system, a system with the most pronounced changes in the thermal conductivity upon cooling, see Figs. 4(a) and 4(b). As pointed out in Sections 3.1 and 3.2, the chemically modified asphaltenes at high asphaltene concentrations are organized in a liquid paraffin in an extended columnar "super-aggregate", see Fig. 8(a) for a typical snapshot of such an aggregate. In fact, the asphaltene molecules in the PAR-ASP-mod-396 system are well separated from the *n*-eicosane chains; this separation also holds after the crystallization has taken place. In the liquid phase the coefficient of the thermal conductivity is found to be six times larger as compared to that of a pure paraffin, see Fig. 4(b). After crystallization, the thermal conductivity of the paraffin-asphaltene and pure paraffin samples are approximately the same (Fig. 4(a)). Thus, it is the columnar asphaltene "super-aggregate" that is responsible for the observed decrease in the thermal conductivity upon cooling.

Due to the π–π interactions, the asphaltene molecules in a stack adopt a parallel arrangement [44,79–81]. To understand the structural changes in the columnar asphaltene aggregate with temperature, we analyzed the overlap between the adjacent asphaltenes within the aggregate. To this end, we calculated the offset distance r_{off} defined as a projection of the distance between the centers of mass of the adjacent planar asphaltenes on the asphaltene's plane. The larger offset distances imply smaller overlaps between the neighboring asphaltene molecules and vice versa. In Fig. 9(a) we show the probability distribution $p(r_{off})$ of the offset distance for three temperatures: 450 K (the liquid phase), 330 K (the liquid phase near the crystallization point), and 250 K (the crystalline phase).

As seen from Fig. 9(a), at T = 450 K, the distribution of the offset distances is rather wide and has a maximum at $r_{off} \approx 0.18$ nm. The visual inspection of a representative extended stack of asphaltene molecules within the aggregate reveals a columnar packing of asphaltenes, see Fig. 8(b). It is this arrangement of asphaltenes that promote the heat transfer.

Upon cooling, the density of a system increases. As the π–π stacking of the asphaltene molecules is mainly governed by the Lennard-Jones interactions [38], the system compression at low temperatures leads to the steric repulsion between atoms of adjacent asphaltenes. Such a repulsion can be minimized by the shifting of neighboring asphaltenes with respect to each other or, in other words, by the increase in the offset distance r_{off}. Indeed, this increase can be witnessed in Fig. 9(a): cooling the paraffin-asphaltene sample results in the narrowing of the probability

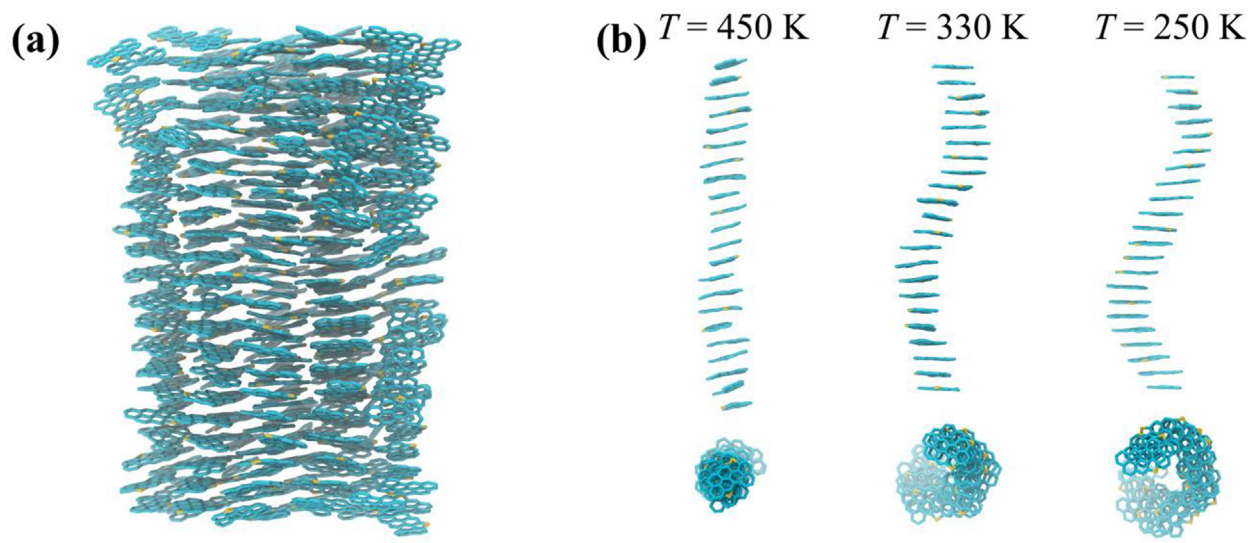

Fig. 8. (a) The typical snapshot of the columnar asphaltene aggregate at T = 450 K. (b) The side- and top-views on the extended columnar stacks of asphaltene at different temperatures. Shown are the results for the CHARMM simulations of the PAR-ASP-mod-396 system.

distribution of offset distances along with the shift of the distribution to larger values. As mentioned above, the increase in the offset distance is directly related to the decrease in the asphaltene overlap, which is known to have a negative impact on the heat transport from one polycyclic core to another [82].

Moreover, the corresponding snapshots of an extended asphaltene stack at low temperatures show dramatic changes in the asphaltenes' structural organization. As seen in Fig. 8(b), an asphaltene stack now has a helix-like shape; the top view of the stack reveals that the asphaltenes are twisted around the long stack axis. We note that this computational finding resembles the results of ref [83], which showed that the discotic liquid crystals were transformed from the columnar hexagonal phase to the columnar helical phase upon cooling.

In addition to the offset distance, we analyzed the temperature-induced changes in the intermolecular radial distribution functions of the asphaltene atoms, see Fig. 9(b). It is seen that the RDF peaks that correspond to the location of the neighboring asphaltene cores are shifted toward the smaller distances upon cooling, indicating thereby the overall compression of a system at low temperatures. Furthermore, the RDF peaks become lower and less pronounced upon cooling, implying that the regularity of the asphaltene arrangement is disrupted.

Overall, our analysis shows that cooling the liquid paraffin-asphaltene samples reduces the overlap of the adjusted asphaltene molecules in an aggregate. In addition, the columnar extended stacks of the chemically modified asphaltenes transform into the helical twisted structures upon cooling. Both these factors disrupt thermal conduction paths of the asphaltenes in paraffin, dramatically weakening the thermal conductivity properties of the crystalline paraffin-asphaltene composite samples.

4. Conclusions

Paraffins, being typical representatives of the organic phase-change materials, are excellent candidates for the use in heat

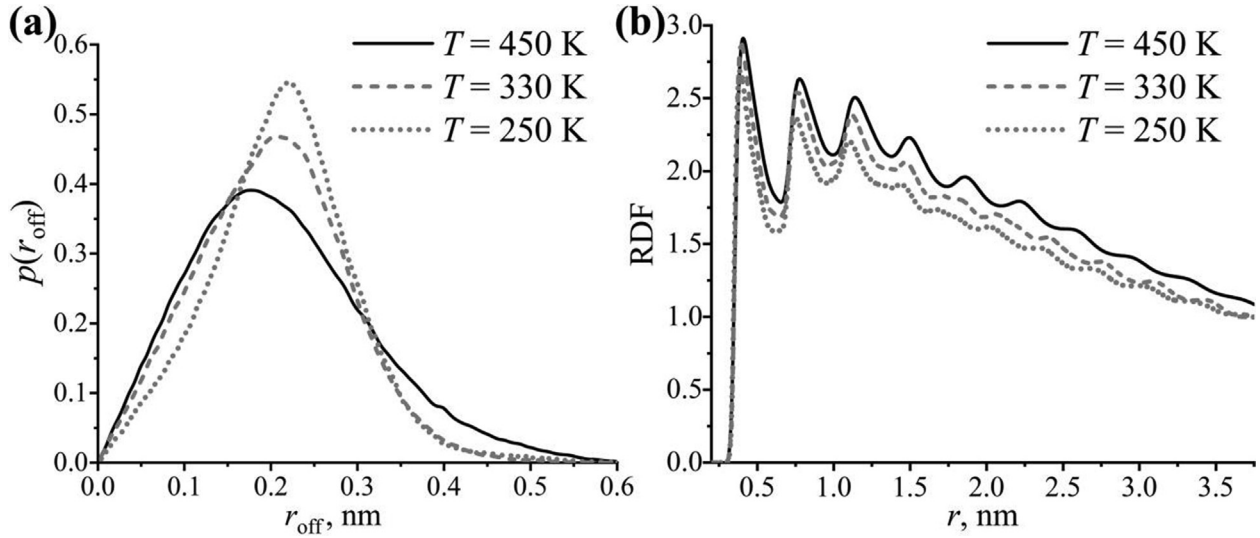

Fig. 9. (a) The probability distribution $p(r_{off})$ of the offset distances between the adjacent asphaltene molecules. (b) The intermolecular radial distribution functions of the asphaltene atoms. Shown are the results for CHARMM simulations of the PAR-ASP-mod-396 system at different temperatures.

storage devices. Paraffins are characterized by the high energy storage density, the thermal and chemical stability, the nontoxicity, and low cost. The transition temperature of paraffins (i.e. the operating temperature range of the corresponding heat storage device) can easily be tuned by varying the average length of *n*-alkane chains that constitute the paraffins. However, the practical application of paraffins is largely limited by their low thermal conductivity, resulting in the low rate of charging and discharging of the paraffin-based heat storage devices. A common approach for enhancing the thermal conductivity consists in adding the substances with high thermal conductivity such as carbon-based nano-additives (graphene and carbon nanotubes). Given that graphene and carbon nanotubes are prohibitively expensive, it is highly desirable to have a cheaper – but still effective – alternative.

In this paper we employed 60 μs-long atomistic computer simulations to probe for the first time the asphaltene molecules as thermal conductivity enhancers of paraffin (*n*-eicosane). Asphaltenes, being natural polycyclic aromatic hydrocarbons, represent a low-cost byproduct of deep oil refining; an asphaltene molecule comprises one or several moderately large polycyclic aromatic cores decorated with short peripheral alkane chains. Our hope was that the π-π interactions between asphaltenes' polycyclic disk-like cores promote the formation of ordered aggregates which could serve as thermal conduction paths, accelerating thereby the heat transfer.

We focused on a simple model asphaltene molecule (one polycyclic aromatic core with peripheral alkane chains) and evaluated the impact of various concentrations of the asphaltenes on the thermal conductivity of liquid and crystalline paraffin. Our computational findings show that the asphaltenes of the considered molecular architecture are not able to improve the thermal conductivity of paraffin. Although the asphaltenes do aggregate, their aggregates are found to be relatively small due to the steric constraints imposed by the peripheral alkane groups of each asphaltene molecule. In the crystalline phase these small asphaltene aggregates disrupt the dense ordered packing of *n*-alkane chains of paraffin, which can even lead to a smaller thermal conductivity compared to that of a pure paraffin. Moreover, some high concentrations of asphaltenes can prevent the crystallization of the paraffin-asphaltene samples. In turn, in a liquid paraffin the asphaltene aggregates do not lead to the noticeable increases in the thermal conductivity due to their small sizes.

As the alkane periphery of asphaltenes are found to limit the π-π stacking between asphaltene's aromatic cores, we also considered the chemically modified asphaltene molecules, in which the peripheral alkane chains were cut off. Experimentally, this could be achieved by cracking (dealkylation) of asphaltenes [47,48]. It turned out that such a chemical modification drastically changed the overall picture. The modified asphaltenes now form the extended columnar aggregates, whose size increases with the asphaltene concentration. These ordered aggregates can serve as efficient thermal conduction paths, enhancing thereby the thermal conductivity of a liquid paraffin. For the highest asphaltene concentration (50 wt%) we found at least a 2-fold increase of the coefficient of thermal conductivity of a liquid paraffin-asphaltene sample. This increase, however, vanishes with the decrease of temperature. A thorough analysis shows that cooling reduces the overlap of adjacent asphaltene molecules in an aggregate. In addition, the columnar extended stacks of chemically modified asphaltenes transform into the helical twisted structures. Both these factors disrupt thermal conduction paths of asphaltenes in paraffin, weakening the heat transfer in crystalline paraffin-asphaltene samples.

Importantly, in our study all the computer simulations were carried out with two different force fields (CHARMM and GAFF). Such an approach allowed us to minimize the possible simulation artifacts and to test the robustness of the computational results against the theoretical models employed. We found that both force fields provided qualitatively similar results. When it comes to the quantitative comparison, the largest difference was observed for the thermal conductivity growth induced by the chemically modified asphaltenes: adding 50 wt% of the modified asphaltenes led to the 6- and 2-fold increase in the thermal conductivity of liquid paraffin in CHARMM and GAFF simulations, respectively. Such a difference is directly linked to the strength of the interactions between asphaltene's aromatic cores in both force fields. For the aromatic core of a considered molecular architecture these interactions turn out to be stronger in the CHARMM force field, so that the corresponding asphaltene aggregates are much more ordered and extended as compared to what is observed in GAFF simulations. Similar extended discotic aggregates were also observed in experiments for coronene molecules [46], whose chemical structure resembles that of modified asphaltenes, i.e. the CHARMM force field could be considered as a better option. However, in the absence of experimental data on chemically modified asphaltenes, a definitive choice of the computational model is currently not possible.

Overall, our computational findings clearly showed that adding chemically modified asphaltene molecules can considerably enhance the thermal conductivity of a liquid paraffin. In practical terms, this implies that these asphaltenes can be used for increasing the rate of discharging of paraffin-based heat storage devices. In particular, at an experimentally feasible concentration of 35 wt%, our computer simulations predict the asphaltene-induced increase in the thermal conductivity of liquid paraffin by 50 – 250 %, depending on a computational model. Given that an increase of tens of percent is regarded as a good outcome for a thermal conductivity enhancer [84,85], the modified asphaltene molecules without peripheral alkane groups should be considered as a promising carbon-based additive for organic phase-change material such as paraffin.

CRediT authorship contribution statement

Artyom D. Glova: Conceptualization, Methodology, Software, Validation, Investigation, Formal analysis, Writing – original draft, Visualization. **Victor M. Nazarychev:** Validation, Investigation, Formal analysis, Writing – review & editing, Visualization. **Sergey V. Larin:** Methodology, Investigation, Writing – review & editing. **Alexey V. Lyulin:** Conceptualization, Methodology, Writing – review & editing, Supervision. **Sergey V. Lyulin:** Conceptualization, Methodology, Writing – review & editing, Supervision. **Andrey A. Gurtovenko:** Conceptualization, Methodology, Validation, Writing – review & editing, Supervision, Project administration, Funding acquisition.

Declaration of Competing Interest

The authors declare that they have no known competing financial interests or personal relationships that could have appeared to influence the work reported in this paper.

Acknowledgements

The authors thank Drs. M. R. Yakubov, S. V. Antonov, and I. V. Volgin for fruitful discussions. This work was supported by the Russian Science Foundation (State Agreement No. 19-13-00178). The simulations were performed using the computational resources of the Institute of Macromolecular Compounds RAS, the equipment of the shared research facilities of HPC computing resources at Lomonosov Moscow State University, the resources of the Federal collective usage center "Complex for Simulation

and Data Processing for Mega-science Facilities" at NRC "Kurchatov Institute" (http://ckp.nrcki.ru/), and the supercomputers at Joint Supercomputer Center of the Russian Academy of Sciences (JSCC RAS).

Appendix A. Supplementary material

Supplementary data to this article can be found online at https://doi.org/10.1016/j.molliq.2021.117112.

References

[1] I. Sarbu, C. Sebarchievici, A comprehensive review of thermal energy storage, Sustainability 10 (2018) 191, https://doi.org/10.3390/su10010191.
[2] M.M. Farid, A.M. Khudhair, S.A.K. Razack, S. Al-Hallaj, A review on phase change energy storage: materials and applications, Energy Convers. Manag. 45 (9-10) (2004) 1597–1615, https://doi.org/10.1016/j.enconman.2003.09.015.
[3] A. Sharma, V.V. Tyagi, C.R. Chen, D. Buddhi, Review on thermal energy storage with phase change materials and applications, Renew. Sustain. Energy Rev. 13 (2) (2009) 318–345, https://doi.org/10.1016/j.rser.2007.10.005.
[4] Z. Khan, Z. Khan, A. Ghafoor, A review of performance enhancement of PCM based latent heat storage system within the context of materials, thermal stability and compatibility, Energy Convers. Manag. 115 (2016) 132–158, https://doi.org/10.1016/j.enconman.2016.02.045.
[5] B. Zalba, J.M. Marín, L.F. Cabeza, H. Mehling, Review on thermal energy storage with phase change: materials, heat transfer analysis and applications, Appl. Therm. Eng. 23 (3) (2003) 251–283, https://doi.org/10.1016/S1359-4311(02)00192-8.
[6] S. Himran, A. Suwono, G.A. Mansoori, Characterization of alkanes and paraffin waxes for application as phase change energy storage medium, Energy Sources 16 (1) (1994) 117–128, https://doi.org/10.1080/00908319408909065.
[7] Y. Lin, Y. Jia, G. Alva, G. Fang, Review on thermal conductivity enhancement, thermal properties and applications of phase change materials in thermal energy storage, Renew. Sustain. Energy Rev. 82 (2018) 2730–2742, https://doi.org/10.1016/j.rser.2017.10.002.
[8] N.I. Ibrahim, F.A. Al-Sulaiman, S. Rahman, B.S. Yilbas, A.Z. Sahin, Heat transfer enhancement of phase change materials for thermal energy storage applications: a critical review, Renew Sustain. Energy Rev. 74 (2017) 26–50, https://doi.org/10.1016/j.rser.2017.01.169.
[9] B.E. Jebasingh, A.V. Arasu, A comprehensive review on latent heat and thermal conductivity of nanoparticle dispersed phase change material for low-temperature applications, Energy Storage Mater. 24 (2020) 52–74, https://doi.org/10.1016/j.ensm.2019.07.031.
[10] S. Wu, T. Yan, Z. Kuai, W. Pan, Thermal conductivity enhancement on phase change materials for thermal energy storage: a review, Energy Storage Mater. 25 (2020) 251–295, https://doi.org/10.1016/j.ensm.2019.10.010.
[11] A.A. Balandin, S. Ghosh, W. Bao, I. Calizo, D. Teweldebrhan, F. Miao, C.N. Lau, Superior thermal conductivity of single-layer graphene, Nano Lett. 8 (3) (2008) 902–907, https://doi.org/10.1021/nl0731872.
[12] M. Amin, N. Putra, E.A. Kosasih, E. Prawiro, R.A. Luanto, T.M.I. Mahlia, Thermal properties of beeswax/graphene phase change material as energy storage for building applications, Appl. Therm. Eng. 112 (2017) 273–280, https://doi.org/10.1016/j.applthermaleng.2016.10.085.
[13] A.A. Balandin, Thermal properties of graphene and nanostructured carbon materials, Nat. Mater. 10 (8) (2011) 569–581, https://doi.org/10.1038/nmat3064.
[14] Sigma-Aldrich, n.d. http://www.sigmaaldrich.com.
[15] O.C. Mullins, The asphaltenes, Annu. Rev. Anal. Chem. 4 (1) (2011) 393–418, https://doi.org/10.1146/annurev-anchem-061010-113849.
[16] K. Akbarzadeh, A. Hammami, A. Kharrat, D. Zhang, S. Allenson, J. Creek, S. Kabir, A. Jamaluddin, A. Marshall, R. Rodgers, O. Mullins, T. Solbakken, Asphaltenes – problematic but rich in potential, Oil F. Rev. (2007) 22–43.
[17] L.V. Meléndez, A. Lache, J.A. Orrego-Ruiz, Z. Pachón, E. Mejía-Ospino, Prediction of the SARA analysis of Colombian crude oils using ATR–FTIR spectroscopy and chemometric methods, J. Pet. Sci. Eng. 90–91 (2012) 56–60, https://doi.org/10.1016/j.petrol.2012.04.016.
[18] S.O. Ilyin, M.P. Arinina, M.Y. Polyakova, V.G. Kulichikhin, A.Y. Malkin, Rheological comparison of light and heavy crude oils, Fuel 186 (2016) 157–167, https://doi.org/10.1016/j.fuel.2016.08.072.
[19] C. Vilas Bôas Fávero, T. Maqbool, M. Hoepfner, N. Haji-Akbari, H.S. Fogler, Revisiting the flocculation kinetics of destabilized asphaltenes, Adv. Colloid Interface Sci. 244 (2017) 267–280, https://doi.org/10.1016/j.cis.2016.06.013.
[20] E. Rogel, C. Ovalles, M. Moir, Asphaltene stability in crude oils and petroleum materials by solubility profile analysis, Energy Fuels 24 (8) (2010) 4369–4374, https://doi.org/10.1021/ef100478y.
[21] H. Wu, M.R. Kessler, Asphaltene: structural characterization, molecular functionalization, and application as a low-cost filler in epoxy composites, RSC Adv. 5 (31) (2015) 24264–24273, https://doi.org/10.1039/C5RA00509D.
[22] H. Wu, V.K. Thakur, M.R. Kessler, Novel low-cost hybrid composites from asphaltene/SBS tri-block copolymer with improved thermal and mechanical properties, J. Mater. Sci. 51 (5) (2016) 2394–2403, https://doi.org/10.1007/s10853-015-9548-1.
[23] M.N. Siddiqui, Studies of different properties of polystyrene-asphaltene composites, Macromol. Symp. 354 (2015) 184–190, https://doi.org/10.1002/masy.201400133.
[24] M.N. Siddiqui, Preparation and properties of polypropylene-asphaltene composites, Polym. Compos. 38 (9) (2017) 1957–1963, https://doi.org/10.1002/pc.23766.
[25] V.Y. Ignatenko, S.V. Antonov, A.V. Kostyuk, N.M. Smirnova, V.V. Makarova, S.O. Ilyin, Composites based on polystyrene and asphaltenes, Russ. J. Appl. Chem. 92 (12) (2019) 1712–1717, https://doi.org/10.1134/S1070427219120125.
[26] V.Y. Ignatenko, A.V. Kostyuk, J.V. Kostina, D.S. Bakhtin, V.V. Makarova, S.V. Antonov, S.O. Ilyin, Heavy crude oil asphaltenes as a nanofiller for epoxy resin, Polym. Eng. Sci. 60 (7) (2020) 1530–1545, https://doi.org/10.1002/pen.25399.
[27] R.E. Abujnah, H. Sharif, B. Torres, K. Castillo, V. Gupta, R.R. Chianelli, Asphaltene as light harvesting material in dye-sensitized solar cell: resurrection of ancient leaves, J. Environ. Anal. Toxicol. 06 (2016), https://doi.org/10.4172/2161-0525.1000345.
[28] E.M. Deemer, R.R. Chianelli, Novel applications with asphaltene electronic structure, in: Modif. asph., InTech, 2018, https://doi.org/10.5772/intechopen.78379.
[29] N.I. Borzdun, R.R. Ramazanov, A.D. Glova, S.V. Larin, S.V. Lyulin, Model carboxyl-containing asphaltenes as potential acceptor materials for bulk heterojunction solar cells, Energy & Fuels. 35 (9) (2021) 8423–8429, https://doi.org/10.1021/acs.energyfuels.1c00253.
[30] D.D. Li, M.L. Greenfield, Chemical compositions of improved model asphalt systems for molecular simulations, Fuel. 115 (2014) 347–356, https://doi.org/10.1016/j.fuel.2013.07.012.
[31] A.D. Glova, I.V. Volgin, V.M. Nazarychev, S.V. Larin, S.V. Lyulin, A.A. Gurtovenko, Toward realistic computer modeling of paraffin-based composite materials: critical assessment of atomic-scale models of paraffins, RSC Adv. 9 (66) (2019) 38834–38847, https://doi.org/10.1039/C9RA07325F.
[32] I.V. Volgin, A.D. Glova, V.M. Nazarychev, S.V. Larin, S.V. Lyulin, A.A. Gurtovenko, Correction: toward realistic computer modeling of paraffin-based composite materials: critical assessment of atomic-scale models of paraffins, RSC Adv. 10 (52) (2020) 31316–31317, https://doi.org/10.1039/D0RA90087G.
[33] V.M. Nazarychev, A.D. Glova, I.V. Volgin, S.V. Larin, A.V. Lyulin, S.V. Lyulin, A.A. Gurtovenko, Evaluation of thermal conductivity of organic phase-change materials from equilibrium and non-equilibrium computer simulations: paraffin as a test case, Int. J. Heat Mass Transf. 165 (2021) 120639, https://doi.org/10.1016/j.ijheatmasstransfer.2020.120639.
[34] S.V. Lyulin, A.D. Glova, S.G. Falkovich, V.A. Ivanov, V.M. Nazarychev, A.V. Lyulin, S.V. Larin, S.V. Antonov, P. Ganan, J.M. Kenny, Computer simulation of asphaltenes, Petroleum Chem. 58 (12) (2018) 983–1004, https://doi.org/10.1134/S0965544118120149.
[35] G. Javanbakht, M. Sedghi, W.R.W. Welch, L. Goual, M.P. Hoepfner, Molecular polydispersity improves prediction of asphaltene aggregation, J. Mol. Liquids 256 (2018) 382–394, https://doi.org/10.1016/j.molliq.2018.02.051.
[36] O.C. Mullins, H. Sabbah, J. Eyssautier, A.E. Pomerantz, L. Barré, A.B. Andrews, Y. Ruiz-Morales, F. Mostowfi, R. McFarlane, L. Goual, R. Lepkowicz, T. Cooper, J. Orbulescu, R.M. Leblanc, J. Edwards, R.N. Zare, Advances in asphaltene science and the Yen-Mullins model, Energy Fuels. 26 (7) (2012) 3986–4003, https://doi.org/10.1021/ef300185p.
[37] M.M. Ramirez-Corredores, Asphaltenes, in: Sci. Technol. Unconv. Oils, Elsevier, 2017, pp. 41–222. https://doi.org/10.1016/B978-0-12-801225-3.00002-4.
[38] Artyom D. Glova, Sergey V. Larin, Victor M. Nazarychev, Josè M. Kenny, Alexey V. Lyulin, Sergey V. Lyulin, Toward predictive molecular dynamics simulations of asphaltenes in toluene and heptane, ACS Omega. 4 (22) (2019) 20005–20014, https://doi.org/10.1021/acsomega.9b02992.
[39] Meena B. Singh, Nakul Rampal, Ateeque Malani, Structural behavior of isolated asphaltene molecules at the oil–water interface, Energy Fuels 32 (8) (2018) 8259–8267, https://doi.org/10.1021/acs.energyfuels.8b01648.
[40] Z. Dong, Z. Liu, P. Wang, X. Gong, Nanostructure characterization of asphalt-aggregate interface through molecular dynamics simulation and atomic force microscopy, Fuel 189 (2017) 155–163, https://doi.org/10.1016/j.fuel.2016.10.077.
[41] Meng Xu, Junyan Yi, Pei Qi, Hao Wang, Mihai Marasteanu, Decheng Feng, Improved chemical system for molecular simulations of asphalt, Energy Fuels 33 (4) (2019) 3187–3198, https://doi.org/10.1021/acs.energyfuels.9b00489.
[42] Todd Emrick, Emily Pentzer, Nanoscale assembly into extended and continuous structures and hybrid materials, NPG Asia Mater. 5 (3) (2013), https://doi.org/10.1038/am.2012.73.
[43] Gediminas Kiršanskas, Qian Li, Karsten Flensberg, Gemma C. Solomon, Martin Leijnse, Designing π -stacked molecular structures to control heat transport through molecular junctions, Appl. Phys. Lett. 105 (23) (2014) 233102, https://doi.org/10.1063/1.4903340.
[44] R.D. Majumdar, T. Montina, O.C. Mullins, M. Gerken, P. Hazendonk, Insights into asphaltene aggregate structure using ultrafast MAS solid-state 1 H NMR spectroscopy, Fuel 193 (2017) 359–368, https://doi.org/10.1016/j.fuel.2016.12.082.
[45] J.A. Duran, Y.A. Casas, Li Xiang, Ling Zhang, Hongbo Zeng, H.W. Yarranton, Nature of asphaltene aggregates, Energy Fuels 33 (5) (2019) 3694–3710, https://doi.org/10.1021/acs.energyfuels.8b03057.
[46] Tobias Wöhrle, Iris Wurzbach, Jochen Kirres, Antonia Kostidou, Nadia Kapernaum, Juri Litterscheidt, Johannes Christian Haenle, Peter Staffeld, Angelika Baro, Frank Giesselmann, Sabine Laschat, Discotic liquid crystals,

Chem. Rev. 116 (3) (2016) 1139–1241, https://doi.org/10.1021/acs.chemrev.5b00190.
[47] Ali H. Alshareef, Khalid Azyat, Rik R. Tykwinski, Murray R. Gray, Measurement of cracking kinetics of pure model compounds by thermogravimetric analysis, Energy Fuels 24 (7) (2010) 3998–4004, https://doi.org/10.1021/ef100437u.
[48] H.M.S. Lababidia, H.M. Sabtia, F.S. AlHumaidan, Changes in asphaltenes during thermal cracking of residual oils, Fuel 117 (2014) 59–67, https://doi.org/10.1016/j.fuel.2013.09.048.
[49] Junmei Wang, Romain M. Wolf, James W. Caldwell, Peter A. Kollman, David A. Case, Development and testing of a general amber force field, J. Comput. Chem. 25 (9) (2004) 1157–1174, https://doi.org/10.1002/jcc.20035.
[50] Jeffery B. Klauda, Richard M. Venable, J. Alfredo Freites, Joseph W. O'Connor, Douglas J. Tobias, Carlos Mondragon-Ramirez, Igor Vorobyov, Alexander D. MacKerell, Richard W. Pastor, Update of the CHARMM all-atom additive force field for lipids: validation on six lipid types, J. Phys. Chem. B 114 (23) (2010) 7830–7843, https://doi.org/10.1021/jp101759q.
[51] Jeffery B. Klauda, Bernard R. Brooks, Alexander D. MacKerell, Richard M. Venable, Richard W. Pastor, An ab initio study on the torsional surface of alkanes and its effect on molecular simulations of alkanes and a DPPC bilayer, J. Phys. Chem. B 109 (11) (2005) 5300–5311, https://doi.org/10.1021/jp0468096.
[52] Pradeep Venkataraman, Kyriakos Zygourakis, Walter G. Chapman, Scott L. Wellington, Michael Shammai, Molecular Insights into glass transition in condensed core asphaltenes, Energy Fuels 31 (2) (2017) 1182–1192, https://doi.org/10.1021/acs.energyfuels.6b02322.
[53] Weiguo Wang, Cooper Taylor, Hui Hu, Kathryn L. Humphries, Arjun Jaini, Michael Kitimet, Thais Scott, Zach Stewart, Kevin John Ulep, Shannon Houck, Adam Luxon, Boyi Zhang, Bill Miller, Carol A. Parish, Andrew E. Pomerantz, Oliver C. Mullins, Richard N. Zare, Nanoaggregates of diverse asphaltenes by mass spectrometry and molecular dynamics, Energy Fuels 31 (9) (2017) 9140–9151, https://doi.org/10.1021/acs.energyfuels.7b01420.
[54] Raphael S. Alvim, Filipe C.D.A. Lima, Verónica M. Sánchez, Thomas F. Headen, Edo S. Boek, Caetano R. Miranda, Adsorption of asphaltenes on the calcite (10.4) surface by first-principles calculations, RSC Adv. 6 (97) (2016) 95328–95336, https://doi.org/10.1039/C6RA19307B.
[55] B. Liu, J. Li, C. Qi, X. Li, T. Mai, J. Zhang, Mechanism of asphaltene aggregation induced by supercritical CO 2: insights from molecular dynamics simulation, RSC Adv. 7 (2017) 50786–50793, https://doi.org/10.1039/C7RA09736K.
[56] Lidiya Gavrilenko, Jeffery B. Klauda, Aggregation of modified hexabenzocoronenes as models for early stage asphaltene self-assembly, Mol. Simul. 44 (12) (2018) 992–1003, https://doi.org/10.1080/08927022.2018.1469752.
[57] Kolawole Sonibare, Lasantha Rathnayaka, Liqun Zhang, Comparison of CHARMM and OPLS-aa forcefield predictions for components in one model asphalt mixture, Constr. Build. Mater. 236 (2020) 117577, https://doi.org/10.1016/j.conbuildmat.2019.117577.
[58] David Van Der Spoel, Erik Lindahl, Berk Hess, Gerrit Groenhof, Alan E. Mark, Herman J.C. Berendsen, GROMACS: fast, flexible, and free, J. Comput. Chem. 26 (16) (2005) 1701–1718, https://doi.org/10.1002/jcc.20291.
[59] Alan W Sousa da Silva, Wim F Vranken, ACPYPE – AnteChamber PYthon Parser interfacE, BMC Res. Notes 5 (1) (2012) 367, https://doi.org/10.1186/1756-0500-5-367.
[60] Junmei Wang, Wei Wang, Peter A. Kollman, David A. Case, Automatic atom type and bond type perception in molecular mechanical calculations, J. Mol. Graph. Model. 25 (2) (2006) 247–260, https://doi.org/10.1016/j.jmgm.2005.12.005.
[61] Jumin Lee, Xi Cheng, Jason M. Swails, Min Sun Yeom, Peter K. Eastman, Justin A. Lemkul, Shuai Wei, Joshua Buckner, Jong Cheol Jeong, Yifei Qi, Sunhwan Jo, Vijay S. Pande, David A. Case, Charles L. Brooks, Alexander D. MacKerell, Jeffery B. Klauda, Wonpil Im, CHARMM-GUI input generator for NAMD, GROMACS, AMBER, OpenMM, and CHARMM/OpenMM simulations using the CHARMM36 additive force field, J. Chem. Theory Comput. 12 (1) (2016) 405–413, https://doi.org/10.1021/acs.jctc.5b00935.
[62] Sunhwan Jo, Taehoon Kim, Vidyashankara G. Iyer, Wonpil Im, CHARMM-GUI: a web-based graphical user interface for CHARMM, J. Comput. Chem. 29 (11) (2008) 1859–1865, https://doi.org/10.1002/jcc.20945.
[63] H.J.C. Berendsen, J.P.M. Postma, W.F. van Gunsteren, A. DiNola, J.R. Haak, Molecular dynamics with coupling to an external bath, J. Chem. Phys. 81 (8) (1984) 3684–3690, https://doi.org/10.1063/1.448118.
[64] Shüichi Nosé, A molecular dynamics method for simulations in the canonical ensemble, Mol. Phys. 52 (2) (1984) 255–268, https://doi.org/10.1080/00268978400101201.
[65] William G. Hoover, Canonical dynamics: equilibrium phase-space distributions, Phys. Rev. A 31 (3) (1985) 1695–1697, https://doi.org/10.1103/PhysRevA.31.1695.
[66] M. Parrinello, A. Rahman, Polymorphic transitions in single crystals: a new molecular dynamics method, J. Appl. Phys. 52 (12) (1981) 7182–7190, https://doi.org/10.1063/1.328693.
[67] B. Hess, P-LINCS: a parallel linear constraint solver for molecular simulation, J. Chem. Theory Comput. 4 (2008) 116–122, https://doi.org/10.1021/ct700200b.
[68] Ulrich Essmann, Lalith Perera, Max L. Berkowitz, Tom Darden, Hsing Lee, Lee G. Pedersen, A smooth particle mesh Ewald method, J. Chem. Phys. 103 (19) (1995) 8577–8593, https://doi.org/10.1063/1.470117.
[69] Steve Plimpton, Fast parallel algorithms for short-range molecular dynamics, J. Comput. Phys. 117 (1) (1995) 1–19, https://doi.org/10.1006/jcph.1995.1039.
[70] Teng Zhang, Tengfei Luo, Role of chain morphology and stiffness in thermal conductivity of amorphous polymers, J. Phys. Chem. B 120 (4) (2016) 803–812, https://doi.org/10.1021/acs.jpcb.5b09955.
[71] Melville S. Green, Markoff random processes and the statistical mechanics of time-dependent phenomena. II. Irreversible processes in fluids, J. Chem. Phys. 22 (3) (1954) 398–413, https://doi.org/10.1063/1.1740082.
[72] Ryogo Kubo, Statistical-mechanical theory of irreversible processes. I. General theory and simple applications to magnetic and conduction problems, J. Phys. Soc. Jpn. 12 (6) (1957) 570–586, https://doi.org/10.1143/JPSJ.12.570.
[73] D. Surblys, H. Matsubara, G. Kikugawa, T. Ohara, Application of atomic stress to compute heat flux via molecular dynamics for systems with many-body interactions, Phys. Rev. E 99 (2019) 051301, https://doi.org/10.1103/PhysRevE.99.051301.
[74] Guadalupe Jiménez-Serratos, Tim S. Totton, George Jackson, Erich A. Müller, Aggregation behavior of model asphaltenes revealed from large-scale coarse-grained molecular simulations, J. Phys. Chem. B. 123 (10) (2019) 2380–2396, https://doi.org/10.1021/acs.jpcb.8b12295.
[75] Nasim Haji-Akbari, Phitsanu Teeraphapkul, Arjames T. Balgoa, H. Scott Fogler, Effect of n-alkane precipitants on aggregation kinetics of asphaltenes, Energy Fuels 29 (4) (2015) 2190–2196, https://doi.org/10.1021/ef502743g.
[76] D. Chen, T.S. Totton, J.W.J. Akroyd, S. Mosbach, M. Kraft, Size-dependent melting of polycyclic aromatic hydrocarbon nano-clusters: a molecular dynamics study, Carbon 67 (2014) 79–91, https://doi.org/10.1016/j.carbon.2013.09.058.
[77] E.I. Griggs, D.W. Yarbrough, Thermal conductivity of solid unbranched alkanes from n-hexadecane to n-eicosane, in: Proceedings of the Southeastern Seminar on Thermal Sciences, North Carolina State University, 1978, pp. 256–257.
[78] Y.L. Rastorguev, G.F. Bogatov, B.A. Grigor'ev, Thermal conductivity of higher n-alkanes, Chem. Technol. Fuels. Oils 10 (1974) 728–732, https://doi.org/10.1007/BF00717208.
[79] Huanjiang Wang, Haiyan Xu, Weihong Jia, Juan Liu, Sili Ren, Revealing the intermolecular interactions of asphaltene dimers by quantum chemical calculations, Energy Fuels 31 (3) (2017) 2488–2495, https://doi.org/10.1021/acs.energyfuels.6b02738.
[80] Kevin Carter-Fenk, John M. Herbert, Electrostatics does not dictate the slip-stacked arrangement of aromatic π–π interactions, Chem. Sci. 11 (26) (2020) 6758–6765, https://doi.org/10.1039/D0SC02667K.
[81] Kevin Carter-Fenk, John M. Herbert, Reinterpreting π-stacking, Phys. Chem. Chem. Phys. 22 (43) (2020) 24870–24886, https://doi.org/10.1039/D0CP05039C.
[82] Minwook Park, Dong-Gue Kang, Hyeyoon Ko, Minwoo Rim, Duy Thanh Tran, Sungjune Park, Minji Kang, Tae-Wook Kim, Namil Kim, Kwang-Un Jeong, Molecular engineering of a porphyrin-based hierarchical superstructure: planarity control of a discotic metallomesogen for high thermal conductivity, Mater. Horizons. 7 (10) (2020) 2635–2642, https://doi.org/10.1039/D0MH00966K.
[83] Ernest Fontes, Paul A. Heiney, Wim H. de Jeu, Liquid-crystalline and helical order in a discotic mesophase, Phys. Rev. Lett. 61 (10) (1988) 1202–1205, https://doi.org/10.1103/PhysRevLett.61.1202.
[84] X. Liu, Z.H. Rao, Experimental study on the thermal performance of graphene and exfoliated graphite sheet for thermal energy storage phase change material, Thermochim. Acta 647 (2017) 15–21, https://doi.org/10.1016/j.tca.2016.11.010.
[85] B.W. Xu, Z.J. Li, Paraffin/diatomite/multi-wall carbon nanotubes composite phase change material tailor-made for thermal energy storage cement-based composites, Energy 72 (2014) 371–380, https://doi.org/10.1016/j.energy.2014.05.049.